Study of the performances of different configurations of seawater desalination with a solar membrane distillation

Samira Ben Abdallah*, Nader Frikha, Slimane Gabsi

Unit of Research: Environment, Catalysis and Analysis Processes, National School Engineers of Gabès, Street Omar Ibn ElKhattab, 6029 Gabès, Tunisia
Email: abdallahsamira@yahoo.com

ABSTRACT

The object of this study is the comparison between two configurations of hollow fiber module for seawater vacuum membrane distillation. The first one is a module membrane in series with a solar compound parabolic collector (CPC). The second configuration is a hollow fiber module integrated in a cylindrical absorber of CPC. A model describing the operation of a hollow fiber module, with and without recycling, will be developed. This model determines the instantaneous variation of the temperature of each element of the installation with the distillate flow variation. A comparison of each module production is carried out. A mathematical model describing the performances of different configurations for membrane hollow fibers shows that: (1) The permeate flow for the integrated configuration is always higher than that of not integrated. It can be multiplied by two and even more. (2) The recycling of concentrate makes it possible to improve the production. This is due to the high level temperature at the exit of the module. (3) The energy recovery from the distillate will make it possible to increase the production and to reduce the plant size.

Keywords: Desalination; Modelling; Configuration; Hollow fiber module; Integrated

1. Introduction

Membrane distillation (MD) is a thermal membrane separation process which uses hydrophobic porous membranes to separate a solution physically. The process driving force is the difference between the vapor pressure between the two sides of the membrane [1,2]. The hydrophobic nature of the membrane prevents liquid solutions from entering its pores due to the surface tension forces. As a result, liquid/vapor interfaces are formed at the entrances of the membrane pores. The principle of separation by MD is based on the liquid/vapour equilibrium which controls the selectivity of the process [3–6].

The principal interests of MD compared to other popular separation processes are the lower operating temperatures than the conventional distillation, the lower operating pressures than the pressure-driven processes, the less demanding membrane mechanical properties and the high rejection factor achieved when solutions containing no-volatile solutes [7,8], as well as the greater contact specific area due to the installation compactnesses, the modularity and the possibility of automating the process easily.

*Corresponding author.

MD system can be classified into 4 different configurations: direct contact MD (DCMD), air-gap MD (AGMD), sweeping gas MD and vacuum MD (VMD). The DCMD, AGMD and VMD are best suited for desalination applications [4,9,10].

We are interested in the VMD. It is an evaporative process which uses a hydrophobic porous membrane, whose function is to separate and put in contact a liquid and a gas phase [11].

The diffusion of the water vapour inside the pores is favoured. In addition, there is no boundary layer on the vacuum side and this implies a decrease in the heat conducted through the membrane. In other words, this configuration combines two advantages: a very low conductive heat loss with a reduced mass transfer resistance [12–14].

In this configuration low pressure or vacuum is applied on the permeate side of the membrane module by means of vacuum pumps. The applied permeate pressure is lower than the saturation pressure of volatile molecules to be separated from the feed solution and condensation which takes place outside the membrane module at temperatures much lower than ambient temperature [14]. So the analysis of the operating conditions shows that the parameter key has a relatively low temperature and pressure. Moreover, the process coupling VMD with a source of energy (solar or geothermal) could compete with reverse osmosis [3,15–18].

Being capable of directly using solar thermal energy, the solar MD desalination system has evolved as a promising green technology for alleviating the water resource problem [16,19]. Saffarini et al. showed that solar heater costs accounted for over 70% of the total cost of all systems [20], suggesting the desirability of using alternative sources of thermal energy, such as waste heat. Therefore to minimize energy, Mericq et al. [9] studied the possibility to submerge the plate membrane in salinity gradient solar ponds (SGSP) and solar collector. The use of solar collector seems to be the most interesting solution and allows a maximum permeate flux of $142 \, \text{L} \, \text{h}^{-1} \, \text{m}^{-2}$ to be reached with permeable membrane [9]. In this work, a comparison study between two configurations of the hollow fiber module integrated or not in the solar collector will be achieved to studying the effect of integration and recycling concentrate on the module production.

2. Material and methods

2.1. Coupling DMV module and compound parabolic collector

The installation is composed of a solar desalination system in series with a tank. This one is fed by an auxiliary flow and a part of concentrate flow (Fig. 1).

The desalination system is composed of a compound parabolic collector (CPC) and a hollow fiber module. The main advantages of the hollow fiber module are: very high packing density and low energy consumption [21].

The hollow fiber module configuration is external-internal. The feed solution flows from outside the hollow fibers and the permeate is collected inside the hollow fibers [21,22].

2.1.1. Module not integrated

For this configuration of the hollow fiber module, the desalination system is composed of a heat-insulated module downstream of CPC absorber. This absorber is assimilated to a cylindrical pipe which we impose a temperature T_{abs} at the wall (Fig. 2).

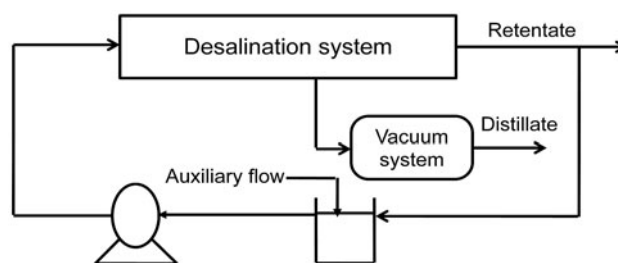In order to compare the two configurations, we considered the same area of the absorber for the two configurations.

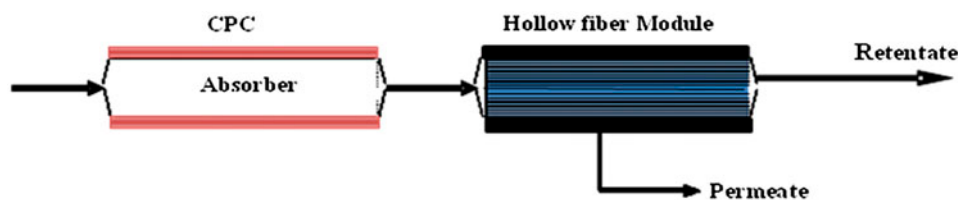Fig. 1. Diagram of the desalination unit.

Fig. 2. Modulate fibres not integrated in the solar collector.

2.1.2. Module integrated in CPC

For this second configuration, the module is placed in the CPC absorber so that the exit module temperature is at the absorbing surface temperature (Fig. 3).

The temperature imposed on the module is the same used for the simulation of not integrated module.

2.2. Modelling

The coupling of mass and heat transfer equations for each element of the unit, module, collector and tank, lead to the establishment of a model describing the unit operation and thus determining the distillate temperature and daily collected quantity.

We developed a model describing the operation of a hollow fiber module coupled with solar energy functioning with concentrated recycling [23].

2.2.1. Membrane module

The heat transfer inside the module is coupled with a mass transfer through the membrane due to the difference in pressure on both sides of the membrane. The establishment of a rigorous model describing the heat and mass transfer inside the hollow fiber module is very complex. To simplify the problem, some assumptions are necessary in order to be able to solve it. First, the angular distance between the fibers is little compared to that radial; we supposed that the fibers placed the ones with the dimensions of the others according to the angular distance by forming an assembly of coaxial cylinders.

Thus, we considered that the internal fiber diameter represents the vacuum thickness compartment. The fiber thickness represents the membrane thickness and the distance between the fibers represents the water thickness compartment. The module consists of a whole coaxial cylinder with alternate compartments water membrane and vacuum membrane, where a mass transfer through the membrane under the gradient pressure effect.

Fig. 4 shows the standard module with three compartments.

The determination of the seawater temperature profile requires developing a heat balance in each water compartment.

The heat balance in water compartment was written as:

$$\rho\, C_{\mathrm{p}}\, V \frac{dT}{dz} = \lambda \left(\frac{1}{r} \frac{d}{dr} \left(r \frac{dT}{dr} \right) + \frac{d^2 T}{dz^2} \right) \tag{1}$$

In general, the conduction heat in the axial direction can be neglected compared to the convection heat flow. The heat balance is reduced to:

$$V \frac{dT}{dz} = \frac{\lambda}{\rho C_{\mathrm{p}}} \frac{1}{r} \frac{d}{dr} \left(r \frac{dT}{dr} \right) \tag{2}$$

The transfer of water molecules in the gas phase through the membrane pores is given by the mechanism of Knudsen diffusion [6,7,13]. The molar water flow J_{v} cross the membrane is described by the following equation:

$$J_{\mathrm{v}} = K_{\mathrm{m}}(P - P_{\mathrm{vacuum}}) \tag{3}$$

The coefficient of the membrane permeability or the Knudson permeability K_{m} can be related to the membrane structural properties such as porosity (ε), the thickness (δ), tortuosity (χ) and the pores radius (r_{p}) and at the membrane interface temperature (T_{i}) [7,15].
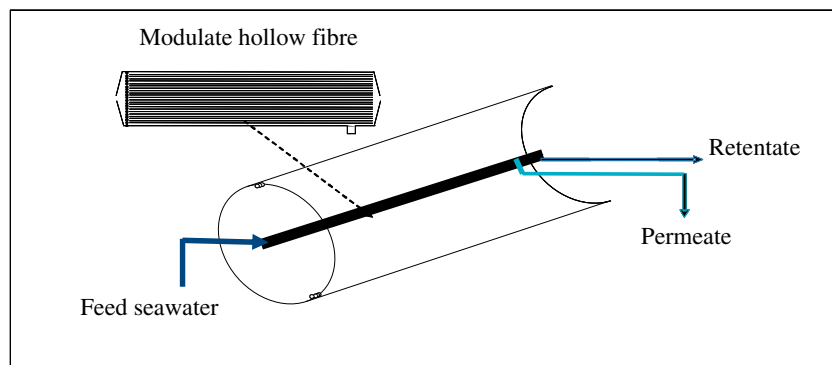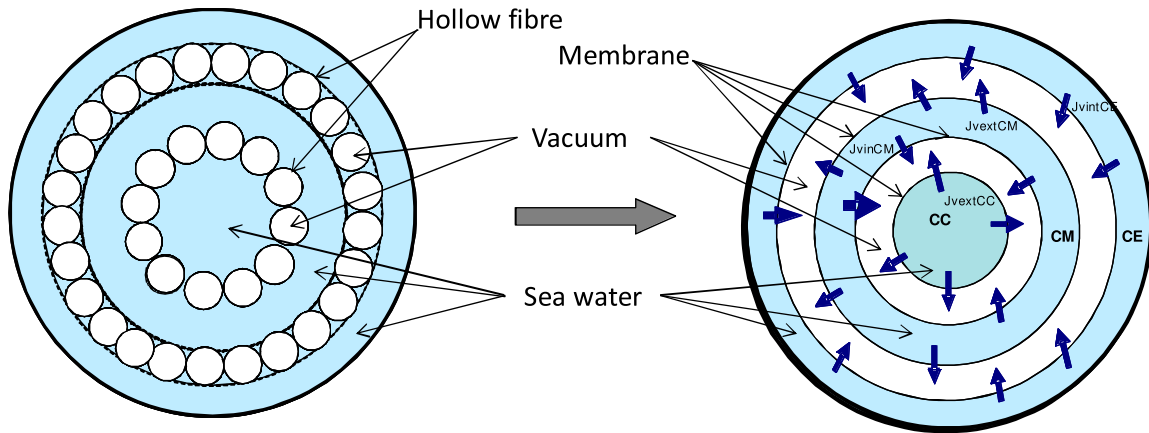

Fig. 3. Modulate hollow fibre integrated in a cylindrical absorber.

CC: Central water compartment. **CE:** External water compartment. **CM:** Water compartment in the medium located between two vacuum compartments

Fig. 4. Cross-section of the module.

$$K_\mathrm{m} = \alpha T_\mathrm{i}^{-0.5} \tag{4}$$

With $\alpha = \dfrac{2\varepsilon r_\mathrm{p}}{3}$ (5)

The Antoine equation:

$$P = \exp\left(c - \frac{d}{T_\mathrm{i} - e}\right) \tag{6}$$

with

$c = 23.1964,\ d = 3816.44,\ e = 46.13$

The evaporated water flux per surface unit is written as:

$$dm_\mathrm{evap} = J_\mathrm{v}\, dS_\mathrm{mem} \tag{7}$$

Then $\rho\, S_\mathrm{p}\, dV = J_\mathrm{v}\, dS_\mathrm{mem}$ (8)

So the velocity expression is:

$$V(z) = \int_0^z \frac{J_\mathrm{v}}{\rho\, S_\mathrm{p}}\, dS_\mathrm{mem} \tag{9}$$

We consider a module with n compartments of water. We have one exterior compartment, one central and $n-2$ compartments located in the middle between two vacuum compartments. The membrane interface temperature is determined by solving the equations describing the mass and heat transfer for each type of compartments.

• For external compartment (CE):

$$\frac{dV}{dz} = \frac{2R_\mathrm{int\ CE}}{\rho\left(R_\mathrm{ext\ CE}^2 - R_\mathrm{int\ CE}^2\right)} J_\mathrm{v\ int\ CE} \tag{10}$$

The velocity is written as:

$$V(z) = V_\mathrm{m} - \frac{2R_\mathrm{int\ CE}}{\rho\left(R_\mathrm{ext\ CE}^2 - R_\mathrm{int\ CE}^2\right)} J_\mathrm{v\ int\ CE}\, z \tag{11}$$

So, the temperature equation can be written as:

$$\rho\, C_\mathrm{p}\left(V_\mathrm{m} - \frac{2R_\mathrm{int\ CE}}{\rho\left(R_\mathrm{ext\ CE}^2 - R_\mathrm{int\ CE}^2\right)} J_\mathrm{v\ int\ CE}\, z\right)\frac{dT}{dz}$$
$$- \lambda \frac{1}{r}\frac{d}{dr}\left(r\frac{dT}{dr}\right) = 0 \tag{12}$$

With $0 \le z \le L$ and $R_\mathrm{int\ CE} \le r \le R_\mathrm{ext\ CE}$

• For the central compartment (CC):

$$\frac{dV}{dz} = \frac{2}{\rho\, R_\mathrm{ext\ CC}} J_\mathrm{vext\ CC} \tag{13}$$

The velocity is written as:

$$V(z) = V_\mathrm{m} - \frac{2}{\rho\, R_\mathrm{ext\ CC}} J_\mathrm{vext\ CC}\, z \tag{14}$$

Then, we obtain the following temperature equation

$$\rho\, C_{\mathrm p}\left(V_{\mathrm m}-\frac{2}{\rho\,R_{\mathrm{ext\ CC}}}J_{\mathrm{vext\ CC}}\,z\right)\frac{dT}{dz}$$
$$-\lambda\frac{1}{r}\frac{d}{dr}\left(r\frac{dT}{dr}\right)=0 \tag{15}$$

With $0\le z\le L$ and $0\le r\le R_{\mathrm{ext\ CC}}$

• For $n-2$ compartments in the medium

The velocity expression for one compartment example is:

$$\frac{dV}{dz}=\frac{2\,(J_{\mathrm{v\ int\ CM}}\,R_{\mathrm{int\ CM}}+J_{\mathrm{vext\ CM}}\,R_{\mathrm{ext\ CM}})}{\rho\left(R_{\mathrm{ext\ CM}}^2-R_{\mathrm{int\ CM}}^2\right)} \tag{16}$$

The velocity is written as:

$$V(z)=V_{\mathrm m}$$
$$-\frac{2\,(J_{\mathrm{v\ int\ CM}}\,R_{\mathrm{int\ CM}}+J_{\mathrm{vext\ CM}}\,R_{\mathrm{ext\ CM}})}{\rho\left(R_{\mathrm{ext\ CM}}^2-R_{\mathrm{int\ CM}}^2\right)}z \tag{17}$$

Then, we obtain the following temperature equation

$$\rho\, C_{\mathrm p}\left(V_{\mathrm m}-\frac{2\,(J_{\mathrm{v\ int\ CM}}\,R_{\mathrm{int\ CM}}+J_{\mathrm{vext\ CM}}\,R_{\mathrm{ext\ CM}})}{\rho\,(R_{\mathrm{ext\ CM}}^2-R_{\mathrm{int\ CM}}^2)}z\right)\frac{dT}{dz}$$
$$-\lambda\frac{1}{r}\frac{d}{dr}\left(r\frac{dT}{dr}\right)=0 \tag{18}$$

With $0\le z\le L$ and $R_{\mathrm{ext\ CM}}\le r\le R_{\mathrm{ext\ CM}}$
The mass transfer equation for each type of compartment gives the distillate flow:

• For CE:

$$D_{\mathrm{CE}}=\int_0^L J_{\mathrm{v\ ext\ CE}}\,2\,\pi\,R_{\mathrm{int\ CE}}dz \tag{19}$$

• For the CC:

$$D_{\mathrm{CC}}=\int_0^L J_{\mathrm{v\ ext\ CC}}\,2\,\pi\,R_{\mathrm{int\ CC}}\,dz \tag{20}$$

• For $n-2$ compartments in the medium located between two vacuum compartments (CM):

$$D_{\mathrm{CM}}=\int_0^L (J_{\mathrm{v\ int\ CM}}\,R_{\mathrm{int\ CM}}+J_{\mathrm{v\ ext\ CM}}\,R_{\mathrm{ext\ CM}})\,2\,\pi dz \tag{21}$$

where
The total distillate flow D is equal to the sum of the various flows in each compartment D_i

$$D=\sum_1^{\mathrm n} D_{\mathrm i} \tag{22}$$

2.2.2. CPC modelling

The absorber is the main component in the CPC, which has the function of absorbing the incident solar radiation, to convert it into heat and to transmit it to a heat transfer fluid.

A heat transfer equation between the absorber and the water leads to a partly differential equation of temperature [24]:

$$\rho_{\mathrm w}C_{\mathrm{Pw}}\pi\frac{D_{\mathrm{iabs}}^2}{4}\frac{dT_{\mathrm w}(z,t)}{dt}$$
$$=-\rho_{\mathrm w}C_{\mathrm{Pw}}\dot V\frac{dT_{\mathrm w}(z,t)}{dz}+q_{\mathrm i}(z,t) \tag{23}$$

$q_{\mathrm i}$ is calculated by the equation Boelter-Dittus for a fully developed flow in a smoother tube:

$$q_{\mathrm i}(z,t)=h_{\mathrm i}\,\pi\,D_{\mathrm{iabs}}\left(T_{\mathrm{abs}}-T_{\mathrm w}\right) \tag{24}$$

With

$$h_{\mathrm i}=0.023\mathrm{Re}^{4/5}\,\mathrm{Pr}^{0.3}\,\frac{K_{\mathrm w}}{D_{\mathrm{iabs}}} \tag{25}$$

So, the temperature equation is as follows:

$$\frac{dT_{\mathrm w}}{dt}=-\frac{4\dot V}{\pi D_{\mathrm{iabs}}^2}\frac{dT_{\mathrm w}}{dz}$$
$$+\frac{4h_{\mathrm c}}{D_{\mathrm{iabs}}\rho_{\mathrm w}C_{\mathrm{Pw}}}\left(T_{\mathrm{abs}}-T_{\mathrm w}\right) \tag{26}$$

Other, the heat balance between the absorber and the environment is described by the following equation:

$$\rho_{\mathrm{abs}}C_{\mathrm{Pabs}}\,\pi\,\frac{(D_{\mathrm{eabs}}^2-D_{\mathrm{iabs}}^2)}{4}\frac{dT_{\mathrm{abs}}(z,t)}{dt}$$
$$=Q_{\mathrm{abs}}(t)-q_{\mathrm i}(z,t)-q_{\mathrm e}(z,t) \tag{27}$$

It is assumed that the transfer between the absorber and the environment in only due to convection:

$$q_e(z,t) = h_e \, \pi \, D_{eabs} \left(T_{abs} - T_{amb} \right) \tag{28}$$

With

$$h_e = 0.023 \, \text{Nu} \, \frac{K_{air}}{D_{eabs}} \tag{29}$$

So, the absorber temperature equation is as follows:

$$\frac{dT_{abs}(z,t)}{dt} = \frac{4 \, h_i \, D_{iabs}}{\rho_{abs} \, C_{Pabs} \left(D_{eabs}^2 - D_{eabs}^2 \right)} \, Q_{abs}(t)$$

$$- \frac{4 \, h_i \, D_{iabs}}{\rho_{abs} \, C_{Pabs} \left(D_{eabs}^2 - D_{eabs}^2 \right)} \left(T_{abs} - T_w \right)$$

$$- \frac{4 \, h_e \, D_{eabs}}{\rho_{abs} \, C_{Pabs} \left(D_{eabs}^2 - D_{eabs}^2 \right)} \left(T_{abs} - T_{amb} \right) \tag{30}$$

The solar radiation $Q_{abs}(t)$ received by the CPC was assumed to follow a sinusoidal law:

$$Q_{abs}(t) = E_{max} \sin \left(\pi \frac{t - t_{sunrise}}{t_{sunset} - t_{sunrise}} \right) \tag{31}$$

2.2.3. Coupling CPC and module modelling

The concentrate flow at the module exit $\dot{m}_S$ is equal to the remaining quantity:

$$\dot{m}_S = \dot{m}_e - \dot{D} \tag{32}$$

Other

$$\dot{m}_S = \dot{m}_{ret} + \omega \, \dot{m}_S \tag{33}$$

The recycling ratio is expressed by:

$$\omega = \frac{\dot{m}_S - \dot{m}_{ret}}{\dot{m}_S} \tag{34}$$

The auxiliary mass flow is written as:

$$\dot{m}_{oxy} = (1 - \omega) \, \dot{m}_e + \omega \, \dot{D} \tag{35}$$

Heat balance in the tank:

$$((1 - \omega) \, \dot{m}_e + \omega \, \dot{D}) \, C_p \, T_a + \omega \, (\dot{m}_e - \dot{D}) \, C_p \, T_{ret}$$

$$= \dot{m}_e \, T_r \, C_p + \rho \, C_p \, v \frac{dT_r}{dt} \tag{36}$$

The desalination solar system contains a heating system and a hollow fiber module.which can be integrated/not integrated in the CPC.

The boundary conditions for the two configurations are represented in the following table:

	Not integrated	Integrated
$z = 0$	$T = T_{inlet}$	$T = T_w$
$r = R$	$\frac{dT}{dz} = 0$	$T = T_{abs}$

For the not integrated configuration the module was insulated so as $r = R$ we have $\frac{dT}{dz} = 0$ and the feed temperature was the outlet CPC temperature. Other, for the integrated configuration, the wall module temperature is at the absorber temperature so as $r = R$ we have $T = T_{abs}$ and the feed temperature was the tank temperature.

We developed a calculator program by using the Matlab software computation. This programme solves the differential equation Eqs. (12,15,18). We used the function ode 45 which is based on the Runge and Kutta method. This function is generally used for the lower order systems.

The resolution can be determined by the variation of different temperatures and daily distillate flow.

3. Results and discussion

The hollow fiber module characteristics are selected so that it supports a high temperature at the membrane wall and has a good permeability. Table 1 shows a characteristic of the hollow fiber module.

3.1. Velocity choice

Fig. 5 gives the variation of the distillate flow with the velocity seawater in the compartment.

We noticed that for velocity higher than 0.5 m/s, the distillate flow increases slightly which implies a low increase in the treated water flow.

For a feed velocity 0.5 m/s which corresponds to a feed flow of 268 kg/h, gives a flow of distillate of 3.5 kg/h, while for a velocity of 1 m/s which corresponds to twice the treated water (536 kg/h) the flow of distillate is only multiplied by 1.14. It requires a higher pumping power to ensure a velocity of 1 m/s. It is therefore preferable to work with a velocity of 0.5 m/s.

3.2. Inlet temperature effect

To study the effect of the inlet temperature module on the modulate hollow fiber production, we

determined the distillate flow variation with the feed temperature between 25 and 70℃ (Fig. 6).

The driving force in the DMV is the transmembrane vapor pressure, which can be applied in this case by a pressure difference between the feed and permeate side of the membrane module. The distillate flow increases exponentially with inlet temperature. While increasing the feed side temperature, a monotonic increase in flux with respect to the increase in the bulk phase temperature difference would be observed [3,4,12]. The evaporation pressure increases and the permeability (K_m) decreased slightly then k_m is proportional to $T^{-0.5}$. This implies that for a fixed vacuum, the partial pressures and permeate flow difference increases for the two configurations. To a temperature at the inlet of 50℃, the permeate flow to the integrated configuration reached 5 kg/h whereas the not integrated configuration does not exceed the 3 kg/h. This difference is due necessarily to the heat input of the wall. Fig. 7 represents the variation exit

Table 1
Characteristics of hollow fibre module

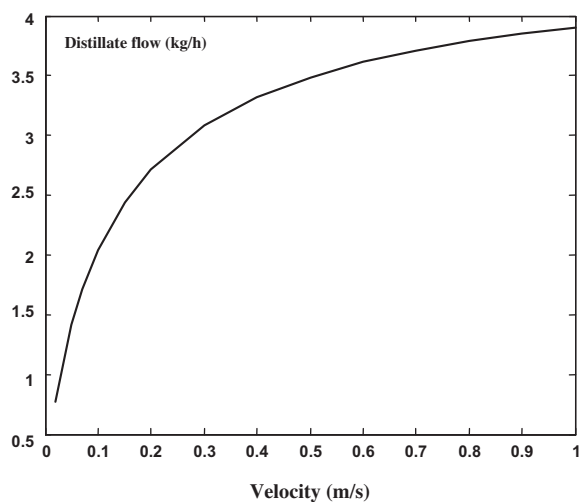| Nature	PVDF
Intenal fibre diameter (mm)	2.6
Membrane thickness (mm)	0.4
Length (m)	1
Fibres number	18
Diameter module (cm)	2
Maximum temperature (℃)	80
Permeability (ms^{-1}) (T_i in K)	$km = 7.8 \times 10^{-6*}\, T_i^{-0.5}$
Vacuum pressure (Pa)	1,000
Water flow rate (m/s)	$0,1 \leq v \leq 1$

temperature for the two configurations according to the feed temperature module.

The module exit temperature increases according to the feed temperature. The variation is not linear. The shapes of the two curves are similar. But, the difference between the two curves decreases when the inlet temperature increases. For the not integrated module the exit temperature is always lower than the feed temperature. Whereas the module exit temperature integrated is practically always higher than that at the entry, this one is favourable for an integrated module functioning with recycling, by taking account of the concentrate heat recovered quantity.

The distillate flow recovered for the hollow fiber integrated module is more significant than that of the module which is not integrated (Table 2). This difference is justified by the fact that the integrated module into a heat source in more which increases the temperature inside the module consequently the distillate flow produces.

The effect of the integration of the hollow fiber module in the solar collector on the production of the module without recycling does not exceed 20% of the flow produced by the fiber module that is not integrated.

The integration of the hollow fiber module in the absorber increases the production of the module by increasing the level of temperature within the module. But, there are energy losses at the exit of the module since the exit temperature of the module for the two configurations remains higher than the ambient temperature.
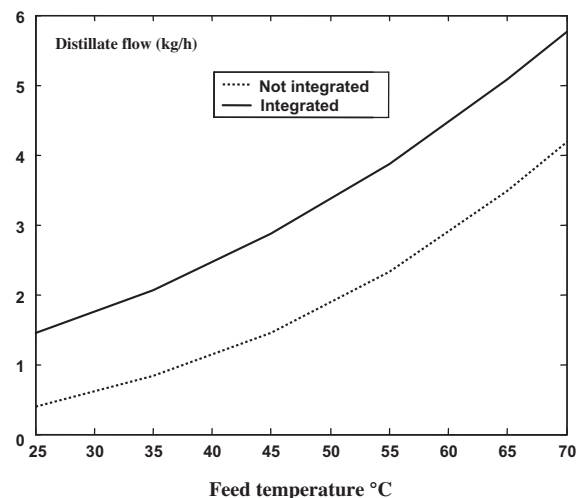

Fig. 5. Variation of the distillate flow vs. velocity ($T_{inlet} = 65$℃).

Fig. 6. Variation of the distillate flow at the module exit vs. the inlet temperature ($v_m = 0.5$ m/s; $D_{modulates} = 2$ cm; 3 water compartments, Tw = 120℃ for integrated).
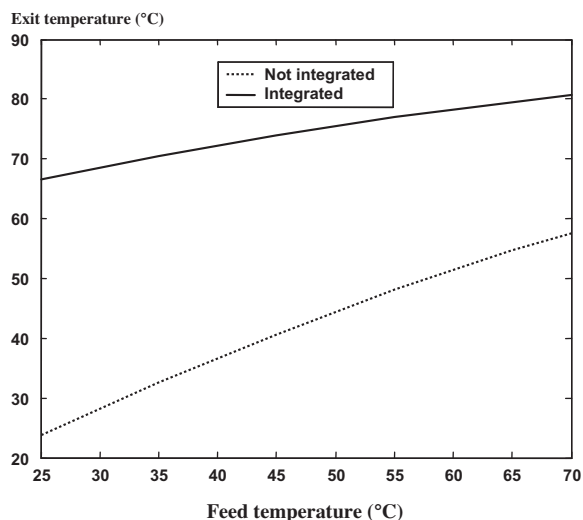
Fig. 7. Variation of the module exit temperature vs. the feed temperature (V_m=0.5 m/s; $D_{modulates}$ = 2 cm; 3 water compartments).

3.3. Hollow fiber module coupled with CPC

The first step of the simulation was the determination of the absorber temperature variation. Fig. 8 shows daily variation of the absorber temperature. It reaches a maximum of 115°C at noon. The feed absorber temperature was 25°C.

Fig. 9 presents a daily variation of the exit absorber and the exit module temperatures. The daily temperature variation follows the same profile as the wall temperature. For the not integrated module the exit absorber temperature was the feed module temperature. After heating in the absorber, the feed module temperature reaches values much lower than those of the integrated module. The temperature gradient between the feed and exit module is nearly the same during the day. The temperature rise of the absorber is due to the wall temperature imposed. This rise does not exceed 4°C at mid-day. The feed module temperature does not exceed 37°C, whereas for the integrated module the exit temperature reaches a maximum of 63°C at noon. The difference between the two temperatures exceeds 20°C. We note that the exit module temperature for the both configurations is always higher than the feed module temperature which gives us the idea of recycling a quantity of concentrate.

Table 2
Comparison of two modules configurations without recycling

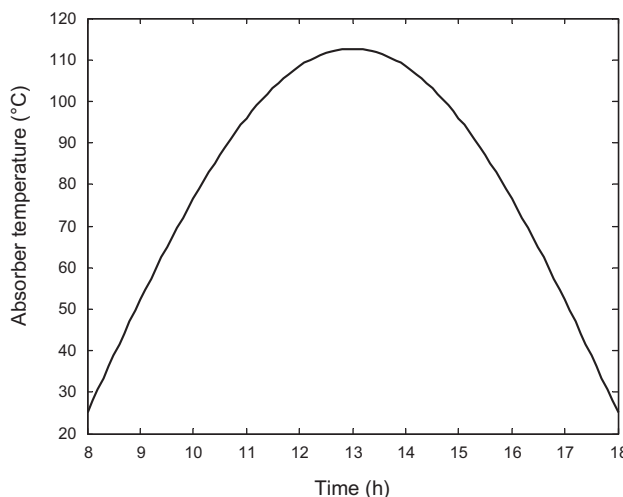| Modulate hollow fibres integrated	Modulate fibres not integrated
Distillate flow = 5 kg/h	Distillate flow = 3.5 kg/h

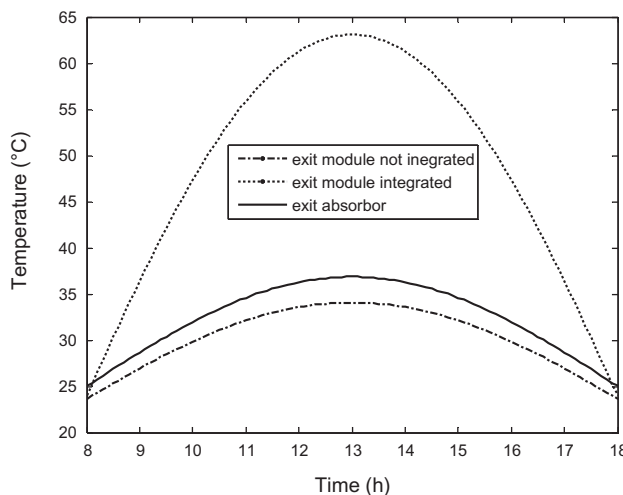Fig. 8. Variation of the daily absorber temperature.

Fig. 9. Variation of the daily exit absorber and module temperature.

The instantaneous variation of the distillate flow for the two configurations is represented in Fig. 10. The flow of distillate increases according to the feed module temperature. It reaches a maximum between 13 and 14 h.

To compare the two configurations of the fiber module we calculate the daily distillate quantity produced for the same operating conditions. The results obtained are illustrated in Table 3. The distillate quantity produces by the module not integrated with total recycling represents almost thrice the production of this module without recycling. The operation of the desalination unit with recycling improves its energy effectiveness, thus its daily production.
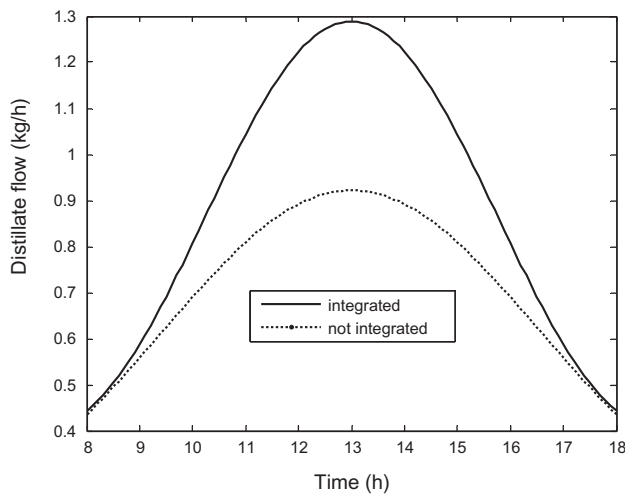
Fig. 10. Instantaneous variation of the distillate flow for two configurations without recycling.

Table 3
Comparison between two modules configurations with recycling

Hollow fiber module	Not integrated	Integrated
Daily module production without recycling	7.27 kg	9.07 kg
Daily module production with recycling	16.27 kg	38.75 kg

The integrated module production with recycling is more than the double of this not integrated. The integration of the hollow fiber module in the solar collector with recycling improve the desalination unit performance. The daily production of the module integrated with recycling is more than the double of that of the not integrated module.

4. Conclusion

A mathematical model describing the performances of different configurations for membrane hollow fibers shows that:

• The permeate flow for the integrated configuration is always higher than that of not integrated. It can be multiplied by two and even more.
• The concentrate recycling makes it possible to improve the production. This is due at the high level temperature at the exit of the module.

• The energy recovery from the distillate will make it possible to increase the production and to reduce the installation size.
• When the membrane is immersed in the collector the production decreases, when the number of water compartment increases. It is thus preferable to choose a standard module of three water compartment and to multiply these modules according to the requirements while keeping a reasonable absorber diameter to avoid too large CPC. It is necessary to study the combination of these modules for scale-up.
• The simulation of the production with type's days will make it possible to determine the real production. This simulation will be more realistic on a simulation all the year with real data weather of the weather station of the region of Gabes, Sfax, etc.

Nomenclature

C_p	—	the specific heat capacity of the water
D	—	the total distillate flow
D_{iabs}	—	the inner diametre of the absorber
D_{eabs}	—	the external diametre of the absorber
dS_{mem}	—	the elementary membrane surface
E_{max}	—	the maximum solar irradiance received during the day
ext	—	external
h_i	—	the heat convection coefficient
int	—	interior
K_{air}	—	the air thermal conductivity
K_m	—	the Knudson permeability
K_w	—	the water thermal conductivity
L	—	module length
$\dot{m}_{oxy}$	—	auxiliary feed mass flow
$\dot{m}_e$	—	module feed mass flow
$\dot{m}_{ret}$	—	mass flow of concentrate
$\dot{m}_s$	—	he exit mass flow
Pr	—	Prandtl number
P_{vacuum}	—	vacuum pressure
Re	—	Reynolds number
r_p	—	pores radius
S_p	—	water flow section
T_{abs}	—	the absorber temperature
T_w	—	the water temperature
T_a	—	the ambient temperature
T_r	—	the tank temperature
T_{ret}	—	the v concentrate temperature
$t_{sunrise}$	—	the time of sunrise
t_{sunset}	—	the time of sunset
V_m	—	the avrage velocity
v	—	the tank volume

ω	—	recycling ratio
χ	—	membrane tortuosity
δ	—	membrane thickness
ε	—	membrane porosity
λ	—	the water conductivity
ρ	—	the water density

References

[1] X. Yanga, R. Wanga, L. Shi, A.G. Fane, M. Debowski, Performance improvement of PVDF hollow fiber-based membrane distillation process, J. Membr. Sci. 369 (2011) 437–447.

[2] R.B. Saffarini, E.K. Summers, H.A. Arafat, J.H. Lienhard, Technical evaluation of stand-alone solar powered membrane distillation systems, Desalination 286 (2012) 332–341.

[3] N. Couffin, C. Cabassud, V. Lahoussine-Turcaud, A new process to remove halogenated VOCs for drinking water production: vacuum membrane distillation, Desalination 117 (1998) 233–245.

[4] M.S. El-Bourawi, Z. Ding, R. Ma, M. Khayet, A framework for better understanding membrane distillation separation process, J. Membr. Sci. 285 (2006) 4–29.

[5] S. Al-Obaidani, E. Curcio, F. Macedonio, G. Di Profio, H. Al-Hinai, E. Drioli, Potential of membrane distillation in seawater desalination: thermal efficiency, sensitivity study and cost estimation, J. Membr. Sci. 323 (2008) 85–98.

[6] K.W. Lawson, D.R. Lloyd, Membrane distillation, J. Membr. Sci. 124 (1997) 1–25.

[7] M. khayet, Membranes and theoretical modeling of membrane distillation: A review, Adv. Colloid Interface Sci. 164 (2011) 56–88.

[8] S. Adnan, M. Hoang, H. Wang, Z. Xie, Commercial PTFE membranes for membrane distillation application: Effect of microstructure and support material, Desalination 284 (2012) 297–308.

[9] J.P. Mericq, S. Laborie, C. Cabassud, Evaluation of systems coupling vacuum membrane distillation and solar energy for sea water desalination, Chem. Eng. J. 166 (2011) 596–606.

[10] E. Curcio, E. Drioli, Membrane distillation and related operations: A review, Sep. Purif. Rev. 34 (2005) 35–86.

[11] D. Wirth, Etude de la distillation pour le dessalement de l'eau de mer, Thèse de Doctorat, Institut National des Sciences Appliquées de [Study of distillation to desalinate seawater, Thesis, National Institute of Applied Sciences], Toulouse, 2002.

[12] A. Alkhudhiri, N. Darwish, N. Hilal, Membrane distillation: A comprehensive review, Desalination 287 (2012) 2–18.

[13] J.I. Mengual, M. Khayet, M.P. Godino, Heat and mass transfer in vacuum membrane distillation, Int. J. Heat Mass Transfer 47 (2004) 865–875.

[14] M. Khayet, T. Matsuura, Membrane Distillation: Principle and Applications, Elsevier, The Netherlands, 2011, p. 325.

[15] D. Wirth, C. Cabassud, Water desalination using membrane distillation: Comparison between inside/out and outside/in permeation, Desalination 147 (2002) 139–145.

[16] H. Chang, S. Lyu, C. Tsai, Y. Chen, T. Cheng, Y. Chou, Experimental and simulation study of a solar thermal driven membrane distillation desalination process, Desalination 286 (2012) 400–411.

[17] A. Zrelli, B. Chaouchi, S. Gabsi, Simulation of vacuum membrane distillation coupled with solar energy: Optimization of the geometric configuration of a helically coiled fiber, Desalin. Water Treat. 36 (2011) 41–49.

[18] M. Khayet, Solar desalination by membrane distillation: Dispersion in energy consumption analysis and water production costs (A review), Desalination 308 (2012) 89–101.

[19] A. Cipollina, M.G. Di Sparti, A. Tamburini, G. Micale, Development of a membrane distillation module for solar energy seawater desalination, Chem. Eng. Res. Des. 90 (2012) 2101–2121.

[20] R.B. Saffarini, E.K. Summersb, H.A. Arafata, Economic evaluation of stand-alone solar powered membrane distillation systems, Desalination 299 (2012) 55–62.

[21] A. Alkhudhiri, N. Darwish, N. Hilal, Membrane distillation: A comprehensive review, Desalination 287 (2012) 2–18.

[22] C. Cabassud, D. Wirth, Membrane distillation for water desalination: How to choose an appropriate membrane? Desalination 157 (2003) 307–314.

[23] S. Ben Abdallah, N. Frikha, B. Chaouchi, S. Gabsi, Modélisation du transfert thermique et de matière dans module de fibers creuses intégré dans un capteur solaire cylindro-parabolique, Récents Progrès en Génie des Procédés, Numéro 98–2009, 2–910239-72-1, Ed. SFGP [Modeling of heat and mass transfer in a hollow fibers module integrated in a parabolic trough solar collector, SFGP], Paris.

[24] W. Chekirou, N. Boukheit, T. Kerbache, Various modes of heat transfer in an absorber of a cylindrical parabolic solar concentrator, ICRESD-07, Tlemcen, 2007, pp. 21–28.